

1 **Mitigating NO_x emissions does not help alleviate wintertime particulate pollution in**
2 **Beijing-Tianjin-Hebei (BTH), China**

3
4 Xia Li^{1,5}, Naifang Bei², Bo Hu³, Yuan Wang⁴, Suixin Liu¹, Jiarui Wu¹, Yuepeng Pan³, Tianxue Wen³, Zirui
5 Liu³, Lang Liu¹, Ruonan Wang¹, Min Zuo¹, Zhenxing Shen², Junji Cao^{1,6}, Xuexi Tie¹, Luisa T. Molina⁷,
6 and Guohui Li^{1,6*}

7
8 ¹Key Lab of Aerosol Chemistry and Physics, SKLLQG, Institute of Earth Environment, Chinese Academy
9 of Sciences, Xi'an, Shaanxi, 710061, China

10 ²School of Human Settlements and Civil Engineering, Xi'an Jiaotong University, Xi'an, Shaanxi, 710049,
11 China

12 ³State Key Laboratory of Atmospheric Boundary Layer Physics and Atmospheric Chemistry, Institute of
13 Atmospheric Physics, Chinese Academy of Sciences, Beijing, 100029, China

14 ⁴Division of Geological and Planetary Sciences, California Institute of technology, Pasadena, CA 91125,
15 USA

16 ⁵University of the Chinese Academy of Sciences, Beijing, 100049, China

17 ⁶CAS Center for Excellence in Quaternary Science and Global Change, Xi'an, Shaanxi, 710061, China

18 ⁷Molina Center for Energy and the Environment, La Jolla, California, CA 92037, USA

19
20 * **Correspondence to:** Guohui Li (ligh@ieecas.cn)

21

22 **Abstract:** Stringent mitigation measures have reduced wintertime $PM_{2.5}$ concentrations by
23 42.2% from 2013 to 2018 in the BTH. The observed nitrate aerosols have not exhibited a
24 significant decreasing trend and constituted a major fraction (about 20%) of the total $PM_{2.5}$,
25 although the surface-measured NO_2 level has decreased by over 20%. It still remains elusive
26 about contributions of nitrogen oxides (NO_x) emissions mitigation to the nitrate and $PM_{2.5}$
27 level. The WRF-Chem model simulations of a persistent haze episode in January 2019 in the
28 BTH reveal that NO_x emissions mitigation does not help lower wintertime nitrate and $PM_{2.5}$
29 concentrations under current conditions in the BTH, because the substantial O_3 increase
30 induced by NO_x mitigation offsets the HNO_3 loss and enhances sulfate and secondary organic
31 aerosols formation. Our results are further consolidated by occurrence of the severe PM
32 pollution in the BTH during the COVID-19 outbreak with a significant reduction of NO_2 .

33

34 **Plain Language Summary:** Rapid industrialization and urbanization have caused severe
35 particulate matter (PM) pollution in winter in Beijing-Tianjin-Hebei (BTH) region, China.
36 Strict mitigation measures have been conducted to improve the air quality, but heavy PM
37 pollution still frequently engulfs the region. The observed nitrate aerosols have not exhibited
38 a significant decreasing trend and constituted a major fraction (about 20%) of the $PM_{2.5}$,
39 although the surface-measured NO_2 level has decreased by over 20%. We quantify the
40 contributions of nitrogen oxides (NO_x) emissions mitigation to the nitrate and $PM_{2.5}$ level in
41 the BTH using a fully coupled WRF-Chem model and further explore how to efficiently
42 alleviate nitrate aerosols under current situations. Our simulations of a persistent heavy haze
43 episode in January 2019 in the BTH reveal that NO_x emissions mitigation does not help
44 lower wintertime nitrate and $PM_{2.5}$ concentrations under current conditions in the BTH and
45 mitigation of NH_3 emissions constitutes the priority measure to effectively decrease the
46 nitrate and $PM_{2.5}$ level.

47

48 1. Introduction

49 The severe and persistent particulate matter (PM) pollution in China is attributed to a synergy
50 of massive anthropogenic emissions and unfavorable synoptic situations, as well as the
51 topography (An et al., 2019; Bei et al., 2016a, b; Long et al., 2016). Great efforts have been
52 made by the Chinese central and local governments to mitigate anthropogenic emissions
53 since 2013 with release of “Air Pollution Prevention and Control Action Plan” (APPCAP) (Li
54 et al., 2019; Zhang et al., 2019). Although anthropogenic emissions of major air pollutants,
55 including sulfur dioxide (SO₂), nitrogen oxides (NO_x), black carbon (BC) and organic carbon
56 (OC) have decreased considerably since 2013 (Zhang et al., 2019; Zheng et al., 2019),
57 persistent and heavy PM pollution still frequently engulfs the Beijing-Tianjin-Hebei (BTH)
58 during wintertime, and observations have revealed that nitrate aerosols concentration has
59 progressively increased in recent several years and constituted a major fraction of PM_{2.5} in
60 the BTH (Sun et al., 2015; Tao et al., 2017; Zhang et al., 2015). It still remains elusive about
61 the contribution of NO_x emissions mitigation to the nitrate and PM_{2.5} level.

62 Nitrate aerosols are formed via nitrous acid (HNO₃) to balance inorganic cations in the
63 particle phase, and the reaction of NO₂ with OH to form HNO₃ and with NO₃ to form N₂O₅
64 constitute the major HNO₃ formation pathway in the atmosphere (Liu et al., 2019). Hence,
65 the nitrate formation is not only dependent on its precursor (NO_x) and inorganic cations (such
66 as NH₄⁺), also significantly influenced by the atmospheric oxidizing capability (AOC) which
67 is mainly determined by O₃ and its photochemical derivative OH, as well as existence of
68 sulfate aerosols (Brasseur et al., 1999; Seinfeld and Pandis, 2006). Therefore, effective
69 mitigation of the nitrate aerosols is still challenging considering the complexity of its
70 formation process.

71 In the present study, we report analyses of nitrate measurements in the BTH during
72 wintertime, and perform simulations of a persistent and heavy PM pollution episode in

73 January 2019 using a fully coupled WRF-Chem model to quantitatively estimate
 74 contributions of NO_x emissions mitigation to the nitrate and PM_{2.5} level and seek an efficient
 75 measure to further alleviate PM pollution in the BTH under current situation.

76

77 **2. WRF-Chem model and configurations**

78 The WRF-Chem (Weather Research and Forecasting model coupled with Chemistry) model
 79 (Fast et al., 2006; Grell et al., 2005) modified by Li et al. (2010; 2011a, b; 2012) is used in
 80 the present study to simulate the particulate pollution episode. The wet and dry deposition of
 81 aerosols follows the method used in the CMAQ (Community Multiscale Air Quality Model)
 82 module (Binkowski and Roselle, 2003) and Wesely (1989), respectively. The photolysis rates
 83 are calculated using the FTUV (Fast Radiation Transfer Model), considering both the aerosol
 84 and cloud effects on photolysis (Li et al., 2005, 2011b; Tie et al., 2003). The inorganic
 85 aerosols are calculated using ISORROPIA (Version 1.7) (Nenes et al., 1998). Besides the SO₂
 86 gas-phase oxidations by OH and sCl, a SO₂ heterogeneous reaction parameterization is
 87 adopted in the model, in which the SO₂ oxidation in aerosol water by O₂ catalyzed by Fe³⁺ is
 88 limited by mass transfer resistances in the gas-phase and gas-particle interface (Li et al.,
 89 2017). The secondary organic aerosol (SOA) is predicted using the volatility basis-set (VBS)
 90 modeling method, with contributions from glyoxal and methylglyoxal (Volkamer et al., 2007;
 91 Zhao et al., 2006).

92 In the present study, the WRF-Chem model adopts one grid with horizontal resolution of 6
 93 km (301 × 301 grid points) centered at 38.0°N, 116.0°E (See Figure S1), and 35 sigma
 94 vertical levels with a stretched vertical grid with spacing ranging from 30 m near the surface,
 95 to 500 m at 2.5 km and 1 km above 14 km. The meteorological initial and boundary
 96 conditions are from the NCEP (National Centers for Environmental Prediction) 1° × 1°
 97 reanalysis data, and the chemical initial and boundary conditions are interpolated from the 6 h

98 output of WACCM (Whole Atmosphere Community Climate Model) (Marsh et al., 2013;
 99 Neale et al., 2013). The spin-up time of the WRF-Chem model is 100 hours. The SAPRC-99
 100 (Statewide Air Pollution Research Center, version 1999) chemical mechanism is used in
 101 simulations. The anthropogenic emission inventory used in this study is developed by Zhang
 102 et al. (2009) and Li et al. (2017). The biogenic emissions are calculated online using the
 103 MEGAN (Model of Emissions of Gases and Aerosol from Nature) developed by Guenther et
 104 al. (2006). More detailed model configurations (Table S1) and monitoring data are provided
 105 in *SI Appendix*.

106

107 **3. Results and discussion**

108 **3.1 Variations of air pollutants and aerosol species from 2013 to 2018 in the BTH**

109 Aggressive emission mitigation measures have been carried out in the BTH to decrease air
 110 pollutants since implementation of the “Action Plan” in 2013 (Zhang et al., 2019; Zheng et
 111 al., 2019). Table 1 shows comparisons of the average mass concentrations of air pollutants
 112 during wintertime (referred as to the period from 1 December of the year to 28 February of
 113 the next year) in the BTH from 2013 to 2018. The wintertime SO₂ level has been remarkably
 114 decreased by around 78.3% from 2013 to 2018, and the average PM_{2.5} concentration has
 115 decreased from 153.0 to 88.5 μg m⁻³, or by 42.2%. However, the O₃ concentration displays an
 116 increasing trend, with the enhancement of around 30.3%. Besides, NO₂ concentration
 117 exhibits a slow decreasing trend compared to SO₂, reduced by about 22.0%.

118 Although the wintertime PM_{2.5} concentrations in 2018 have decreased substantially compared
 119 to that in 2013, the occurrence frequency with daily PM_{2.5} concentrations exceeding 75 μg
 120 m⁻³ in the winter of 2018 is about 53.3%, showing persistent particulate pollution in the BTH.
 121 Figure 1 shows the variations of the filter measured average concentrations and percentage of
 122 the PM_{2.5} constituents at an urban site in Beijing from 2013 to 2018 during wintertime

123 pollution days with $\text{PM}_{2.5}$ concentrations exceeding $75 \mu\text{g m}^{-3}$. The average wintertime $\text{PM}_{2.5}$
 124 concentration at the site in Beijing decreases from $170.4 \mu\text{g m}^{-3}$ in 2013 to $108.3 \mu\text{g m}^{-3}$ in
 125 2018, reduced by about 36.4% (See Figure S2), which is primarily contributed by decreases
 126 in sulfate (51.6%), unspecified constituents (mainly mineral dust, 47.1%), organic aerosols
 127 (41.0%), ammonium (37.5%), and nitrate (12.5%). However, the black carbon concentration
 128 increases from 2.9 to $4.3 \mu\text{g m}^{-3}$, with an enhancement of 48.3%, which is likely caused by
 129 the rapid growth of vehicles in Beijing.

130 Figure 2 presents variations of wintertime sulfate, nitrate, and ammonium concentrations
 131 from 2014 to 2018 in Tianjin, Tangshan, Baoding, and Shijiazhuang in the BTH when the
 132 $\text{PM}_{2.5}$ level exceeds $75 \mu\text{g m}^{-3}$. Generally, the wintertime sulfate concentrations exhibit a
 133 decreasing trend in the four cities, particularly in Shijiazhuang with the sulfate reduction of
 134 about 27.4%. However, the nitrate and ammonium concentrations do not display a decreasing
 135 trend, and their contributions to $\text{PM}_{2.5}$ have increased from 11.1% to 18.9% and 5.9% to 10.1%
 136 on average in the four cities, respectively (See Figure S3). Due to lack of effective mitigation
 137 measures for NH_3 , the NH_3 emissions in China still remain stable since 2010 (Zheng et al.,
 138 2019). Therefore, when the metal cation (mainly contained in mineral dust) decreases, NH_3
 139 becomes the dominant contributor of cation to balance anion in the particle phase. Although
 140 sulfate aerosols have decreased in the four cities from 2014 to 2018, the ammonium
 141 concentration does not decrease or even increase due to decreased competence of metal
 142 cation and/or increased nitrate concentrations.

143

144 **3.2 Contributions of NO_x emissions mitigation to nitrate and $\text{PM}_{2.5}$ level in the BTH**

145 The NO_x emissions have been effectively mitigated since 2013 in China (Zheng et al. 2019)
 146 and the observed wintertime NO_2 concentrations have decreased by more than 20% in the
 147 BTH from 2013 to 2018 (Table 1). However, nitrate concentrations do not exhibit an evident

148 decreasing trend in the BTH and have become a major fraction of PM_{2.5} in the BTH with
149 contributions of around 20% in 2018 (Figure 1b and S3). Therefore, simulations of a
150 persistent and heavy particulate pollution episode from 29 December 2018 to 29 January
151 2019 in the BTH have been performed using the WRF-Chem model to quantitatively evaluate
152 contributions of NO_x emissions mitigation to nitrate and PM_{2.5} concentrations and investigate
153 how to effectively alleviate nitrate aerosols. In the base simulation with the emission
154 inventory of the base year of 2018 (F_BASE), the model performs reasonably well in
155 simulating air pollutants (PM_{2.5}, O₃, NO₂, and SO₂), sulfate, nitrate, ammonium and organic
156 aerosols and NH₃. See *SI Appendix* for detailed model validation and quantitative statements
157 of model biases (Figure S4-S7).

158 Pan et al. (2016b) have redefined the importance of nitrate aerosols during PM pollution and
159 indicated that controlling NO_x emissions should be a priority in mitigating the serious air
160 pollution. Previous studies have also shown that decreasing NO_x might represent a positive
161 feedback mechanism to reduce the conversion of primary gas pollutants into secondary
162 aerosols (He et al., 2014; Ma et al., 2010; Xu et al., 2015; Wang et al., 2014). Therefore, a
163 sensitivity simulation is firstly conducted in the present study, in which the NO_x emission in
164 the base year of 2013 is used (F_EM13). Compared to F_EM13, on average in the BTH, the
165 NO₂ concentration in F_BASE decreases by around 17.1% but the O₃ concentration increases
166 by 44.2%, which is generally consistent with the observed NO₂ and O₃ trend from 2013 to
167 2018 (Table 1). However, the average PM_{2.5} concentration in F_BASE is 91.8 μg m⁻³, 2.9%
168 higher than that in F_EM13 (Figure 3a). The PM_{2.5} enhancement in F_BASE against
169 F_EM13 is contributed by the increase in secondary aerosols, i.e., sulfate (0.5 μg m⁻³), nitrate
170 (0.9 μg m⁻³), ammonium (0.3 μg m⁻³), and SOA (0.9 μg m⁻³).

171 In order to further assess the impact of NO_x emissions mitigation on the nitrate and PM_{2.5}
172 level in the BTH, the first sensitivity scenario is designed, in which the NO_x emission in

173 F_BASE is reduced from 10% to 50% with a 10% interval. As shown in Figure 3a, the
 174 variations in PM_{2.5} concentration are not as expected, with an average enhancement of about
 175 3.2% (3.0 μg m⁻³) in the BTH when NO_x emissions are reduced by 50%. Although the NO₂
 176 level is decreased monotonically from 6.4% to 40.0% in the BTH with NO_x emissions
 177 decreased from 10% to 50% (Figure 3b), the nitrate concentration increases by 1.1% and then
 178 decreases by 10.3%. Additionally, the SOA, sulfate, and ammonium concentrations are
 179 increased from 3.3% to 10.9%, 4.4% to 26.7%, and 1.9% to 6.3% in the BTH, respectively
 180 (Figure 3a).

181 Therefore, mitigation of NO_x emissions is not beneficial to the air quality at present during
 182 wintertime in the BTH (Figure 3c-3d). Decreasing NO_x emissions does not proportionally
 183 reduce the nitrate concentrations, and particularly enhances formation of sulfate, ammonium,
 184 and SOA, which is primarily caused by the increase in O₃ concentrations (Figure 3b). In
 185 winter in the BTH, the weak insolation significantly decrease photolysis and slow the O₃
 186 formation. During PM pollution period, the lower atmosphere is stable or stagnant, which is
 187 quite favorable for accumulation of air pollutants. The titration of NO_x (mainly NO)
 188 emissions remarkably influence the O₃ level in the PBL. Figure S8 shows the variations of
 189 observed O₃ and NO₂ concentrations as a function of the PM_{2.5} level over all the monitoring
 190 sites in the BTH during the wintertime from 2013 to 2018. With deterioration of PM
 191 pollution, the O₃ concentration decreases but it is opposite for the NO₂ concentration.
 192 Therefore, when the NO_x emissions are decreased from 10% to 50%, the O₃ concentration is
 193 increased from 11.8% to 83.8% in the BTH (Figure 3b). Increased O₃ concentrations enhance
 194 the AOC, not only promoting the SOA and sulfate formation, but also accelerating conversion
 195 of NO₂ to HNO₃ to counterbalance HNO₃ decrease due to mitigation of NO_x emissions.

196 Our results on contributions of NO_x emission mitigation to PM_{2.5} concentrations are also
 197 supported by occurrence of the severe PM pollution in the BTH during outbreak of the

198 Coronavirus Disease 2019 (COVID-19) pandemic with a significant reduction of NO₂. Due
199 to the outbreak of COVID-19, the nationwide preventive lockdown has been carried out since
200 late January 2020 in China, by shutdown of commercial activities and restrictions of
201 population movement. The nationwide lockdown has lasted for more than three weeks and
202 caused remarkable reductions in emissions of air pollutants (Huang et al., 2020; Le et al.,
203 2020; Shi and Brasseur, 2020). Observations from the Tropospheric Monitoring Instrument
204 (TROPOMI) have shown a more than 70% decrease of the column-integrated NO₂ amount
205 during the lockdown period in 2020 over eastern China, compared to that in the same time
206 period in 2019 (Le et al., 2020). Surface measurements have also revealed that the NO₂
207 concentrations have decreased by about 60% between the period 1-22 January 2020 and the
208 period 23 January-29 February 2020 in northern China (Shi and Brasseur, 2020). However,
209 several severe PM pollution events have still occurred in the BTH, with the maximum daily
210 PM_{2.5} concentration exceeding 250 µg m⁻³ in Beijing, although the observed NO₂ level has
211 decreased substantially. Therefore, additional two sensitivity experiments have been devised
212 based on F_BASE, in which the NO_x emissions are further decreased by 60% and 80% to
213 represent variations of the NO_x emission mitigation during the lockdown period. When the
214 NO_x emissions are decreased from 60% to 80%, the NO₂ concentrations in the BTH are
215 reduced from 51.0% to 75.7% compared to those in F_BASE (Figure 3a), which is within the
216 range of the observed NO₂ variation due to the nationwide lockdown. However, the PM_{2.5}
217 level is increased by 2.2% with a 60% reduction of NO_x emissions and decreased by 3.2%
218 with an 80% reduction of NO_x emissions (Figure 3a), showing the significant NO_x emissions
219 reduction does not help lower the PM_{2.5} level during the lockdown period in the BTH. The
220 main reason is that the substantial increase in O₃ concentrations (more than 100%) causes
221 enhancement of SOA and sulfate to offset the nitrate loss.

222

223 **3.3 Priority measure to alleviate wintertime PM pollution in the BTH under current** 224 **situation**

225 Apparently, mitigation of NO_x emissions alleviates O₃ titration during wintertime in the BTH,
226 increasing O₃ concentrations and further the AOC to enhance formation of secondary
227 aerosols. Therefore, decreasing the AOC might effectively lower the nitrate and PM_{2.5} level
228 in the BTH. The second sensitivity scenario is therefore designed, in which the VOCs
229 emission in F_BASE is reduced from 10% to 50% with a 10% interval to lower the O₃
230 concentration. With a 50% reduction of VOCs emissions, the O₃ concentration is decreased
231 by 19.6% in the BTH (See Figure S9b), showing considerable weakening of the AOC.
232 However, the decreases in sulfate, nitrate, and ammonium concentrations are not substantial,
233 only about 13.0%, 18.6%, and 6.1%, respectively (See Figure S9a). The SOA concentration
234 is decreased by about 37.6%, caused to a large degree by the reduction of SOA precursors.
235 Overall, the decrease in PM_{2.5} concentration is not significant (See Figure S9c-9d), around
236 6.9% (6.3 μg m⁻³) in the BTH, when VOCs emissions are reduced by 50%.

237 As a large agricultural country, China produces a huge amount of NH₃ emissions, with
238 agricultural activities accounting for more than 80% (Huang et al., 2012; Paulot et al., 2014;
239 Zhang et al., 2018). Recent studies have pointed out that NH₃ plays an important role in the
240 PM_{2.5} formation and NH₃ control has been advocated as a potential measure by policy makers,
241 given that atmospheric NH₃ facilitates secondary inorganic aerosol formation, i.e.,
242 ammonium sulfate/bisulfate and ammonium nitrate (Fu et al., 2017; Guo et al., 2018; Weber,
243 et al., 2016). Figure S9 presents the pattern comparisons of simulated and measured
244 near-surface NH₃ mass concentrations averaged during January 2019. Compared with
245 measurements, the WRF-Chem model reasonably well simulates the spatial distributions of
246 the NH₃ mass concentrations in the BTH. The NH₃ level is quite high in the plain region of
247 the BTH, with mass concentrations exceeding 5 μg m⁻³. It is well known that the major

248 source of NH₃ is agricultural activities, mainly including livestock and fertilizer use (Huang
 249 et al., 2012; Streets et al., 2003). Additionally, nonagricultural sources (e.g., vehicles, coal
 250 combustion, etc.) are also responsible for the high NH₃ emissions in China, especially in
 251 urban areas (Chang et al., 2016; Pan et al., 2016a).

252 Thus, we have further performed the third sensitivity scenario, in which the NH₃ emission in
 253 F_BASE is reduced from 10% to 50% with a 10% interval. With a 50% reduction of NH₃
 254 emissions, the nitrate and ammonium concentrations are decreased by 34.5% and 36.5% in
 255 the BTH (Figure 4a), respectively. The sulfate concentrations are also reduced by 6.5%,
 256 which is mainly caused by the loss of aerosol liquid water due to decrease in nitrate and
 257 ammonium aerosols (Wu et al., 2019). The SOA concentration in the BTH is slightly
 258 decreased by 0.1% when the NH₃ emissions are reduced by 10% and then increased from 0.1%
 259 to 0.6% when the NH₃ emissions are reduced from 20% to 50%. The PM_{2.5} decrease is about
 260 12.3% (11.3 μg m⁻³) in the BTH (Figure 4c-4d), when NH₃ emissions are reduced by 50%,
 261 showing mitigating NH₃ emissions is much more effective to reduce PM pollution in the
 262 BTH than NO_x and VOCs emissions.

263

264 **4. Conclusions**

265 The Chinese government has made great efforts to mitigate emissions of primary PM, SO₂ and
 266 NO_x to alleviate PM pollution since 2013. The observed near-surface wintertime
 267 concentrations of PM_{2.5}, SO₂, and NO₂ have decreased by 42.2%, 78.3% and 22.0% from
 268 2013 to 2018 in the BTH, respectively, but persistent PM pollution still frequently occurs.
 269 Observations show that nitrate aerosols have not exhibited a significant decreasing trend and
 270 play an increasing role in PM pollution during wintertime in the BTH, with a PM_{2.5}
 271 contribution of about 20%. Our sensitivity simulations of a persistent heavy PM pollution
 272 episode in January 2019 in the BTH reveal that NO_x emissions mitigation does not help

273 lower nitrate and $\text{PM}_{2.5}$ concentrations during wintertime. A 50% reduction of NO_x emissions
274 only decreases nitrate mass by 10.3% but increases $\text{PM}_{2.5}$ concentrations by around 3.2%
275 because the O_3 increase induced by NO_x mitigation offsets the loss of HNO_3 and enhances
276 sulfate and SOA formation. Our results are also consolidated by occurrence of server PM
277 pollutions in the BTH during the COVID-19 outbreak when the NO_x emissions have been
278 remarkably reduced and the observed NO_2 level has decreased by more than 60%.

279 Although the emissions reduction of VOCs has been proposed to be particularly important to
280 mitigate PM pollution, our results reveal that a 50% reduction in VOCs emissions decreases
281 $\text{PM}_{2.5}$ concentrations by around 7% in the BTH. However, when NH_3 emissions are reduced
282 by 50%, the $\text{PM}_{2.5}$ level is decreased by about 12%, mainly caused by substantial decreases in
283 nitrate and ammonium aerosols. Therefore, we suggest that, in addition to primary PM
284 emissions, mitigating NH_3 emissions is the priority measure to effectively alleviate PM
285 pollution during wintertime in the BTH under the current situation.

286

287 **Acknowledgments.** This work is financially supported by the Strategic Priority Research
288 Program of Chinese Academy of Sciences (XDB40030203), the National Key R&D Plan
289 (2017YFC0210000), and National Research Program for Key Issues in Air Pollution Control
290 (DQGG0105).

291

292 **References**

- 293 An, Z. S., Huang, R. J., Zhang, R. Y., Tie, X. X., Li, G. H., Cao, J. J., et al. (2019) Severe haze in northern
 294 China: A synergy of anthropogenic emissions and atmospheric processes. *Proceedings of the National*
 295 *Academy of Sciences of the United States of America*, 116(18), 8657-8666.
 296 <https://doi.org/10.1073/pnas.1900125116>
- 297 Bei, N. F., Li, G. H., Huang, R. J., Cao, J. J., Meng, N., Feng, T., et al. (2016a) Typical synoptic situations
 298 and their impacts on the wintertime air pollution in the Guanzhong basin, China. *Atmospheric*
 299 *Chemistry and Physics*, 16(11), 7373-7387. <https://doi.org/10.5194/acp-16-7373-2016>
- 300 Bei, N. F., Xiao, B., Meng, N., & Feng, T. (2016b) Critical role of meteorological conditions in a persistent
 301 haze episode in the Guanzhong basin, China. *Science of the Total Environment*, 550, 273-284.
 302 <https://doi.org/10.1016/j.scitotenv.2015.12.159>
- 303 Binkowski, F. S., & Roselle, S. J. (2003) Models-3 Community Multiscale Air Quality (CMAQ) model
 304 aerosol component 1. Model description. *Journal of Geophysical Research*, 108(D6), 4183.
 305 <https://doi.org/10.1029/2001JD001409>
- 306 Brasseur, G. P., Orlando, J. J., & Tyndall, G. S. (1999) *Atmospheric Chemistry and Global Change*.
 307 Cambridge, MA: Oxford University Press. <https://doi.org/10.1029/EO080i040p00468-02>
- 308 Chang, Y. H., Zou, Z., Deng, C. R., Huang, K., Collett, J. L., Lin, J., & Zhuang, G. S. (2016) The
 309 importance of vehicle emissions as a source of atmospheric ammonia in the megacity of Shanghai.
 310 *Atmospheric Chemistry and Physics*, 16(5), 3577-3594. <https://doi.org/10.5194/acp-16-3577-2016>
- 311 Elser, M., Huang, R., Wolf, R., Slowik, J. G., Wang, Q., Canonaco, F., et al. (2016) New insights into
 312 PM_{2.5} chemical composition and sources in two major cities in China during extreme haze events
 313 using aerosol mass spectrometry. *Atmospheric Chemistry and Physics*, 16(5), 3207-3225.
 314 <https://doi.org/10.5194/acp-16-3207-2016>
- 315 Fast, J. D., Jr, W. I. G., Easter, R. C., Zaveri, R. A., Barnard, J. C., Chapman, E. G., et al. (2006) Evolution
 316 of ozone, particulates, and aerosol direct radiative forcing in the vicinity of Houston using a fully
 317 coupled meteorology-chemistry-aerosol model. *Journal of Geophysical Research-Atmospheres*,
 318 111(D21), D21305. <https://doi.org/10.1029/2005JD006721>
- 319 Fu, X., Wang, S. X., Xing, J., Zhang, X. Y., Wang, T., & Hao, J. M. (2017) Increasing Ammonia
 320 Concentrations Reduce the Effectiveness of Particle Pollution Control Achieved via SO₂ and NO_x
 321 Emissions Reduction in East China. *Environmental Science & Technology Letters*, 4(6), 221-227.
 322 <https://doi.org/10.1021/acs.estlett.7b00143>
- 323 Gao, M., Carmichael, G. R., Wang, Y., Saide, P. E., Yu, M., Xin, J., et al. (2016) Modeling study of the
 324 2010 regional haze event in the North China Plain. *Atmospheric Chemistry and Physics*, 16(3),
 325 1673-1691. <https://doi.org/10.5194/acp-16-1673-2016>
- 326 Grell, G. A., Peckham, S. E., Schmitz, R., McKeen, S. A., Frost, G., Skamarock, W. C., & Eder, B. (2005)
 327 Fully coupled "online" chemistry within the WRF model. *Atmospheric Environment*, 39(37),
 328 6957-6975. <https://doi.org/10.1016/j.atmosenv.2005.04.027>
- 329 Guenther, A., Karl, T., Harley, P., Wiedinmyer, C., Palmer, P. I., & Geron, C. (2006) Estimates of global
 330 terrestrial isoprene emissions using MEGAN (Model of Emissions of Gases and Aerosols from
 331 Nature). *Atmospheric Chemistry and Physics*, 6, 3181-3210. <https://doi.org/10.5194/acp-6-3181-2006>
- 332 Guo, H., Otjes, R., Schlag, P., Kiendler-Scharr, A., Nenes, A., & Weber, R. J. (2018) Effectiveness of
 333 ammonia reduction on control of fine particle nitrate. *Atmospheric Chemistry and Physics*, 18(16),
 334 12241-12256. <https://doi.org/10.5194/acp-18-12241-2018>
- 335 Guo, S., Hu, M., Zamora, M. L., Peng, J., Shang, D., Zheng, J., et al. (2014) Elucidating severe urban haze
 336 formation in China. *Proceedings of the National Academy of Sciences of the United States of America*,

- 337 *III*(49), 17373-17378. <https://doi.org/10.1073/pnas.1419604111>
- 338 He, H., Wang, Y., Ma, Q., Ma, J., Chu, B., Ji, D., et al. (2014) Mineral dust and NO_x promote the
 339 conversion of SO₂ to sulfate in heavy pollution days. *Scientific Reports*, *4*, 4172.
 340 <https://doi.org/10.1038/srep04172>
- 341 Huang, R. J., Zhang, Y., Bozzetti, C., Ho, K. F., Cao, J. J., Han, Y. M., et al. (2014) High secondary aerosol
 342 contribution to particulate pollution during haze events in China. *Nature*, *514*(7521), 218-222.
 343 <https://doi.org/10.1038/nature13774>
- 344 Huang, X., Ding, A. J., Gao, J., Zheng, B., Zhou, D. R., Qi, X. M., et al. (2020) Enhanced secondary
 345 pollution offset reduction of primary emissions during COVID-19 lockdown in China. *National*
 346 *Science Review*, nwaal137. <https://doi.org/10.31223/osf.io/hvuzy>
- 347 Huang, X., Song, Y., Li, M. M., Li, J. F., Huo, Q., Cai, X. H., et al. (2012) A high-resolution ammonia
 348 emission inventory in China. *Global Biogeochemical Cycles*, *26*, GB1030.
 349 <https://doi.org/10.1029/2011GB004161>
- 350 Le, T. H., Wang, Y., Liu, L., Yang, J. N., Yung, Y. L., Li, G. H., & Seinfeld, J. H. (2020) Unexpected air
 351 pollution with marked emission reductions during the COVID-19 outbreak in China. *Science*,
 352 *369*(6504), 702-706. <https://doi.org/10.1126/science.abb7431>
- 353 Li, G. H., Bei, N. F., Cao, J. J., Huang, R. J., Wu, J. R., Feng, T., et al. (2017) A possible pathway for rapid
 354 growth of sulfate during haze days in China. *Atmospheric Chemistry and Physics*, *17*(5), 3301-3316.
 355 <https://doi.org/10.5194/acp-17-3301-2017>
- 356 Li, G. H., Bei, N. F., Tie, X. X., & Molina, L. T. (2011a) Aerosol effects on the photochemistry in Mexico
 357 City during MCMA-2006/MILAGRO campaign. *Atmospheric Chemistry and Physics*, *11*(11),
 358 5169-5182. <https://doi.org/10.5194/acp-11-5169-2011>
- 359 Li, G. H., Lei, W. F., Bei, N. F., & Molina, L. T. (2012) Contribution of garbage burning to chloride and
 360 PM_{2.5} in Mexico City. *Atmospheric Chemistry and Physics*, *12*(18), 8751-8761.
 361 <https://doi.org/10.5194/acp-12-8751-2012>
- 362 Li, G. H., Lei, W. F., Zavala, M., Volkamer, R., Dusanter, S., Stevens, P., & Molina, L. T. (2010) Impacts
 363 of HONO sources on the photochemistry in Mexico City during the MCMA-2006/MILAGO
 364 Campaign. *Atmospheric Chemistry and Physics*, *10*(14), 6551-6567.
 365 <https://doi.org/10.5194/acp-10-6551-2010>
- 366 Li, G. H., Zavala, M., Lei, W. F., Tsimpidi, A. P., Karydis, V. A., Pandis, S. N., et al. (2011b) Simulations
 367 of organic aerosol concentrations in Mexico City using the WRF- CHEM model during the
 368 MCMA-2006/MILAGRO campaign. *Atmospheric Chemistry and Physics*, *11*(8), 3789-3809.
 369 <https://doi.org/10.5194/acp-11-3789-2011>
- 370 Li, G. H., Zhang, R. Y., Fan, J., & Tie, X. X. (2005) Impacts of black carbon aerosol on photolysis and
 371 ozone. *Journal of Geophysical Research-Atmospheres*, *110*(D23), D23206.
 372 <https://doi.org/10.1029/2005JD005898>
- 373 Li, K., Jacob, D. J., Liao, H., Zhu, J., & Zhai, S. (2019) A two-pollutant strategy for improving ozone and
 374 particulate air quality in China. *Nature Geoscience*, *12*(11).
 375 <https://doi.org/10.1038/s41561-019-0464-x>
- 376 Li, M., Zhang, Q., Kurokawa, J. I., Woo, J. H., He, K., Lu, Z., et al. (2017) MIX: a mosaic Asian
 377 anthropogenic emission inventory under the international collaboration framework of the MICS-Asia
 378 and HTAP. *Atmospheric Chemistry and Physics*, *17*(2), 935-963.
 379 <https://doi.org/10.5194/acp-17-935-2017>
- 380 Liu, L., Wu, J. R., Liu, S. X., Li, X., Zhou, J. M., Feng, T., et al. (2019) Effects of organic coating on the
 381 nitrate formation by suppressing the N₂O₅ heterogeneous hydrolysis: a case study during wintertime
 382 in Beijing-Tianjin-Hebei (BTH). *Atmospheric Chemistry and Physics*, *19*(12), 8189-8207.

- 383 <https://doi.org/10.5194/acp-19-8189-2019>
- 384 Liu, W. J., Shen, G. F., Chen, Y. C., Shen, H. Z., Huang, Y., Li, T. C., et al. (2018) Air pollution and
 385 inhalation exposure to particulate matter of different sizes in rural households using improved stoves
 386 in central China. *Journal of Environmental Science*, 63, 87-95.
 387 <https://doi.org/10.1016/j.jes.2017.06.019>
- 388 Long, X., Tie, X., Cao, J., Huang, R., Feng, T., Li, N., et al. (2016) Impact of crop field burning and
 389 mountains on heavy haze in the North China Plain: a case study. *Atmospheric Chemistry and Physics*,
 390 16(15), 9675-9691. <https://doi.org/10.5194/acp-16-9675-2016>
- 391 Ma, Q., He, H., & Liu, Y. (2010) In situ DRIFTS study of hygroscopic behavior of mineral aerosol.
 392 *Journal of Environmental Science*, 22(4), 555-560. [https://doi.org/10.1016/S1001-0742\(09\)60145-5](https://doi.org/10.1016/S1001-0742(09)60145-5)
- 393 Marsh, D. R., Mills, M., Kinnison, D., Lamarque, J. F., Calvo, N., & Polvani, L. (2013) Climate change
 394 from 1850 to 2005 simulated in CESM1(WACCM). *Journal of Climate*, 26(19), 7372-7391.
 395 <https://doi.org/10.1175/JCLI-D-12-00558.1>
- 396 Neale, R. B., Richter, J., Park, S., Lauritzen, P. H., Vavrus, S. J., Rasch, P. J., & Zhang, M. (2013) The
 397 Mean Climate of the Community Atmosphere Model (CAM4) in Forced SST and Fully Coupled
 398 Experiments. *Journal of Climate*, 26(14), 5150-5168. <https://doi.org/10.1175/JCLI-D-12-00236.1>
- 399 Nenes, A., Pandis, S. N., & Pilinis, C. (1998) ISORROPIA: A new thermodynamic equilibrium model for
 400 multiphase multi-component inorganic aerosols. *Aquatic Geochemistry*, 4, 123-152.
- 401 Pan, Y. P., Tian, S. L., Liu, D. W., Fang, Y. T., Zhu, X. Y., Zhang, Q., et al. (2016a) Fossil Fuel
 402 Combustion-Related Emissions Dominate Atmospheric Ammonia Sources during Severe Haze
 403 Episodes: Evidence from N-15-Stable Isotope in Size-Resolved Aerosol Ammonium. *Environmental
 404 Science & Technology*, 50(15), 8049-8056. <https://doi.org/10.1021/acs.est.6b00634>
- 405 Pan, Y. P., Wang, Y. S., Zhang, J. K., Liu, Z. R., Wang, L. L., Tian, S. L., et al. (2016b) Redefining the
 406 importance of nitrate during haze pollution to help optimize an emission control strategy. *Atmospheric
 407 Environment*, 141, 197-202. <https://doi.org/10.1016/j.atmosenv.2016.06.035>
- 408 Paulot, F., Jacob, D. J., Pinder, R. W., Bash, J. O., Travis, K., & Henze, D. K. (2014) Ammonia emissions
 409 in the United States, European Union, and China derived by high-resolution inversion of ammonium
 410 wet deposition data: Interpretation with a new agricultural emissions inventory (MASAGE_NH₃).
 411 *Journal of Geophysical Research-Atmospheres*, 119(7), 4343-4364.
 412 <https://doi.org/10.1002/2013JD021130>
- 413 Seinfeld, J. H., & Pandis, S. N. (2006) *Atmospheric Chemistry and Physics: From Air Pollution to Climate
 414 Change*, 2nd Edition. New York: John Wiley and Sons Inc. <https://doi.org/10.1063/1.882420>
- 415 Shi, X. Q., & Brasseur, G. P. (2020) The Response in Air Quality to the Reduction of Chinese Economic
 416 Activities During the COVID-19 Outbreak. *Geophysical Research Letters*, 47(11).
 417 <https://doi.org/10.1029/2020GL088070>
- 418 State Council of the People's Republic of China, Notice of the general office of the state council on issuing
 419 the air pollution prevention and control action plan.
 420 http://www.gov.cn/zwqk/2013-09/12/content_2486773.htm. Accessed 4 August 2020.
- 421 Streets, D. G., Bond, T. C., Carmichael, G. R., Fernandes, S. D., Fu, Q., He, D., et al. (2003) An inventory
 422 of gaseous and primary aerosol emissions in Asia in the year 2000. *Journal of Geophysical Research*,
 423 108(D21), 8809. <https://doi.org/10.1029/2002JD003093>
- 424 Sun, Y. L., Wang, Z. F., Du, W., Zhang, Q., Wang, Q. Q., Fu, P. Q., et al. (2015) Long-term real-time
 425 measurements of aerosol particle composition in Beijing, China: seasonal variations, meteorological
 426 effects, and source analysis. *Atmospheric Chemistry and Physics*, 15(17), 10149-10165.
 427 <https://doi.org/10.5194/acp-15-10149-2015>

- 428 Tao, J., Zhang, L., Cao, J. J., & Zhang, R. Y. (2017) A review of current knowledge concerning PM_{2.5}
 429 chemical composition, aerosol optical properties and their relationships across China. *Atmospheric*
 430 *Chemistry and Physics*, 17(15), 9485-9518. <https://doi.org/10.5194/acp-17-9485-2017>
- 431 Tie, X. X., Madronich, S., Walters, S., Zhang, R. Y., Rasch, P., & Collins, W. (2003) Effect of clouds on
 432 photolysis and oxidants in the troposphere. *Journal of Geophysical Research*, 108(D20), 4642.
 433 <https://doi.org/10.1029/2003JD003659>
- 434 Volkamer, R., San Martini, F., Molina, L. T., Salcedo, D., Jimenez, J. L., & Molina, M. J. (2007) A missing
 435 sink for gas-phase glyoxal in Mexico City: formation of secondary organic aerosol. *Geophysical*
 436 *Research Letters*, 34(19), L19807. <https://doi.org/10.1029/2007GL030752>
- 437 Wang, G. H., Zhang, R. Y., Gomez, M. E., Yang, L. X., Zamora, M. L., Hu, M., et al. (2016) Persistent
 438 sulfate formation from London Fog to Chinese haze. *Proceedings of the National Academy of*
 439 *Sciences of the United States of America*, 113(48), 13630-13635.
 440 <https://doi.org/10.1073/pnas.1616540113>
- 441 Wang, Y., Yao, L., Wang, L., Liu, Z., Ji, D., Tang, G., et al. (2014) Mechanism for the formation of the
 442 January 2013 heavy haze pollution episode over central and eastern China. *Science China-Earth*
 443 *Science*, 57(1), 14-25. <https://doi.org/10.1007/s11430-013-4773-4>
- 444 Weber, R. J., Guo, H. Y., Russell, A. G., & Nenes, A. (2016) High aerosol acidity despite declining
 445 atmospheric sulfate concentrations over the past 15 years. *Nature Geoscience*, 9(4), 282-285.
 446 <https://doi.org/10.1038/NGEO2665>
- 447 Wei, S. Y., Shen, G. F., Zhang, Y. Y., Xue, M., Xie, H., Lin, P. C., et al. (2014) Field measurement on the
 448 emissions of PM, OC, EC and PAHs from indoor crop straw burning in rural China. *Environmental*
 449 *Pollution*, 184(SI), 18-24. <https://doi.org/10.1016/j.envpol.2013.07.036>
- 450 Wesely, M. L. (1989) Parameterization of surface resistances to gaseous dry deposition in regional-scale
 451 numerical models. *Atmospheric Environment*, 23(6), 1293-1304.
 452 [https://doi.org/10.1016/0004-6981\(89\)90153-4](https://doi.org/10.1016/0004-6981(89)90153-4)
- 453 Wu, J. R., Bei, N. F., Hu, B., Liu, S. X., Zhou, M., Wang, Q. Y., et al. (2019) Is water vapor a key player of
 454 the wintertime haze in North China Plain? *Atmospheric Chemistry and Physics*, 19(13), 8721-8739.
 455 <https://doi.org/10.5194/acp-2018-1289>
- 456 Xu, W, Luo, X. S., Pan, Y. P., Zhang, L., Tang, A. H., Shen, J. L., et al. (2015) Quantifying atmospheric
 457 nitrogen deposition through a nationwide monitoring network across China. *Atmospheric Chemistry*
 458 *and Physics*, 15(21), 12345-12360. <https://doi.org/10.5194/acp-15-12345-2015>
- 459 Zhang L, Chen, Y. F., Zhao, Y. H., Henze, D. K., Zhu, L. Y., Song, Y., et al. (2018) Agricultural ammonia
 460 emissions in China: Reconciling bottom-up and top-down estimates. *Atmospheric Chemistry and*
 461 *Physics*, 18(1), 339-355. <https://doi.org/10.5194/acp-18-339-2018>
- 462 Zhang, Q., He, K. B., & Huo, H. (2012) Policy: Cleaning China's air. *Nature*, 484(7393), 161-162.
 463 <https://doi.org/10.1038/484161a>
- 464 Zhang, Q., Streets, D. G., & Carmichael, G. R. (2009) Asian emissions in 2006 for the NASA INTEX-B
 465 mission. *Atmospheric Chemistry and Physics*, 9(14), 5131-5153.
 466 <https://doi.org/10.5194/acp-9-5131-2009>
- 467 Zhang, Q., Zheng, Y. X., Tong, D., Shao, M., Wang, S. X., Zhang, Y. H., et al. (2019) Drivers of improved
 468 PM_{2.5} air quality in China from 2013 to 2017. *Proceedings of the National Academy of Sciences of the*
 469 *United States of America*, 116(49), 24463-24469. <https://doi.org/10.1073/pnas.1907956116>
- 470 Zhang, R. Y., Li, G. H., Fan, J. W., Wu, D. L., & Molina, M. J. (2007) Intensification of Pacific storm track
 471 linked to Asian pollution. *Proceedings of the National Academy of Sciences of the United States of*
 472 *America*, 104(13), 5295-5299. <https://doi.org/10.1073/pnas.0700618104>

- 473 Zhang, R. Y., Wang, G. H., Guo, S., Zamora, M. L., Ying, Q., Lin, Y., et al. (2015) Formation of urban fine
 474 particulate matter. *Chemical Reviews*, 115(10), 3803-3855.
 475 <https://doi.org/10.1021/acs.chemrev.5b00067>
- 476 Zhao, B., Wu, W. J., Wang, S. X., Xing, J., Chang, X., Liou, K. N., et al. (2017) A modeling study of the
 477 nonlinear response of fine particles to air pollutant emissions in the Beijing-Tianjin-Hebei region.
 478 *Atmospheric Chemistry and Physics*, 17(19), 12031-12050.
 479 <https://doi.org/10.5194/acp-17-12031-2017>
- 480 Zhao, J., Levitt, N. P., Zhang, R., & Chen, J. (2006) Heterogeneous reactions of methylglyoxal in acidic
 481 media: implications for secondary organic aerosol formation. *Environmental Science & Technology*,
 482 40(24), 7682-7687. <https://doi.org/10.1021/es060610k>
- 483 Zheng, H., Kong, S. F., Wu, F. Q., Cheng, Y., Niu, Z. Z., Zheng, S. R., et al. (2019) Intra-regional transport
 484 of black carbon between the south edge of the North China Plain and central China during winter
 485 haze episodes. *Atmospheric Chemistry and Physics*, 19(7), 4499-4516.
 486 <https://doi.org/10.5194/acp-19-4499-2019>
 487

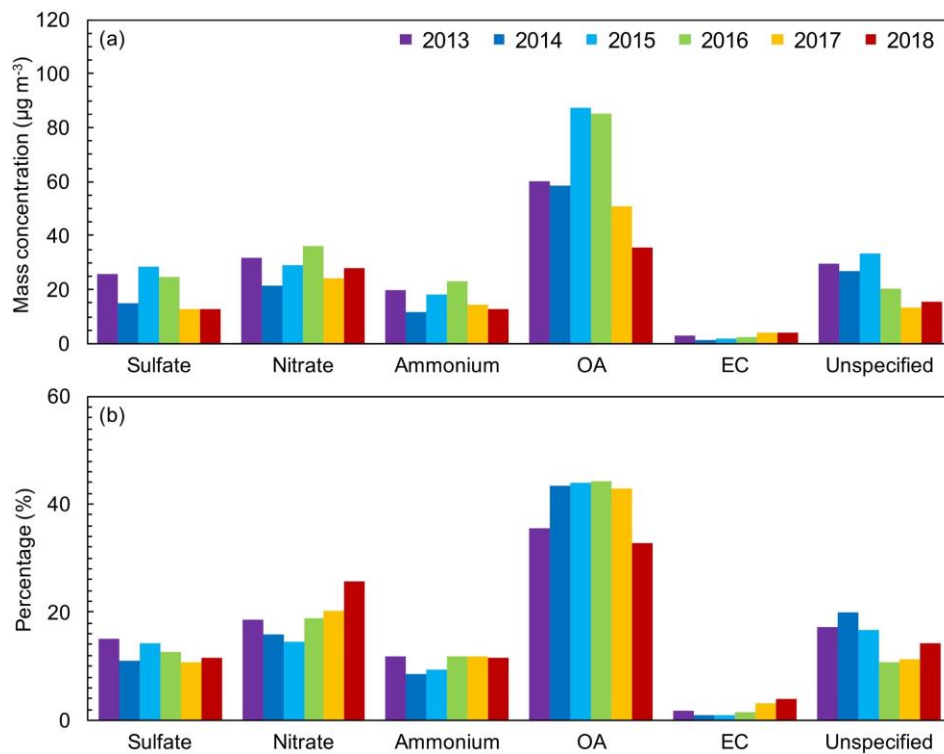
488 Table 1. Comparisons of the average mass concentrations of air pollutants during wintertime
 489 in the BTH from 2013 and 2018.

490

Air pollutants	PM _{2.5} (µg m ⁻³)	O ₃ (µg m ⁻³)	NO ₂ (µg m ⁻³)	SO ₂ (µg m ⁻³)	CO (mg m ⁻³)
2013	153.0	37.9	69.2	108.7	2.6
2014	112.0	42.4	60.3	82.2	2.4
2015	106.8	43.4	63.3	58.3	2.4
2016	136.9	48.2	71.8	52.0	2.6
2017	78.7	47.6	50.6	28.8	1.5
2018	88.5	49.4	54.0	23.6	1.5
Change (%) between 2013 and 2018	-42.2	30.3	-22.0	-78.3	-42.3

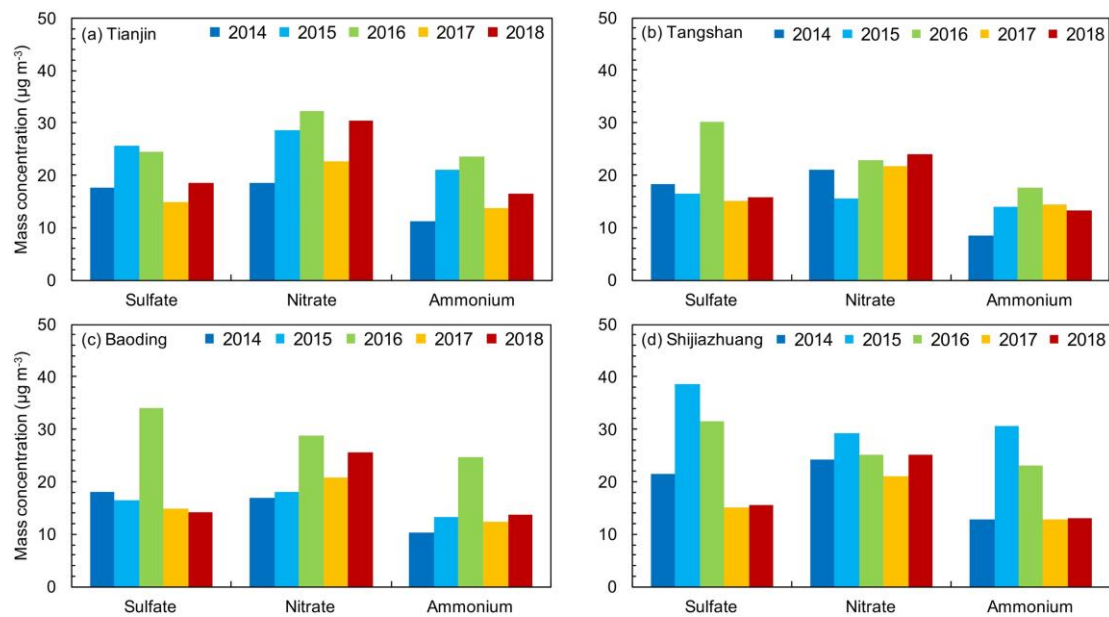
491

492



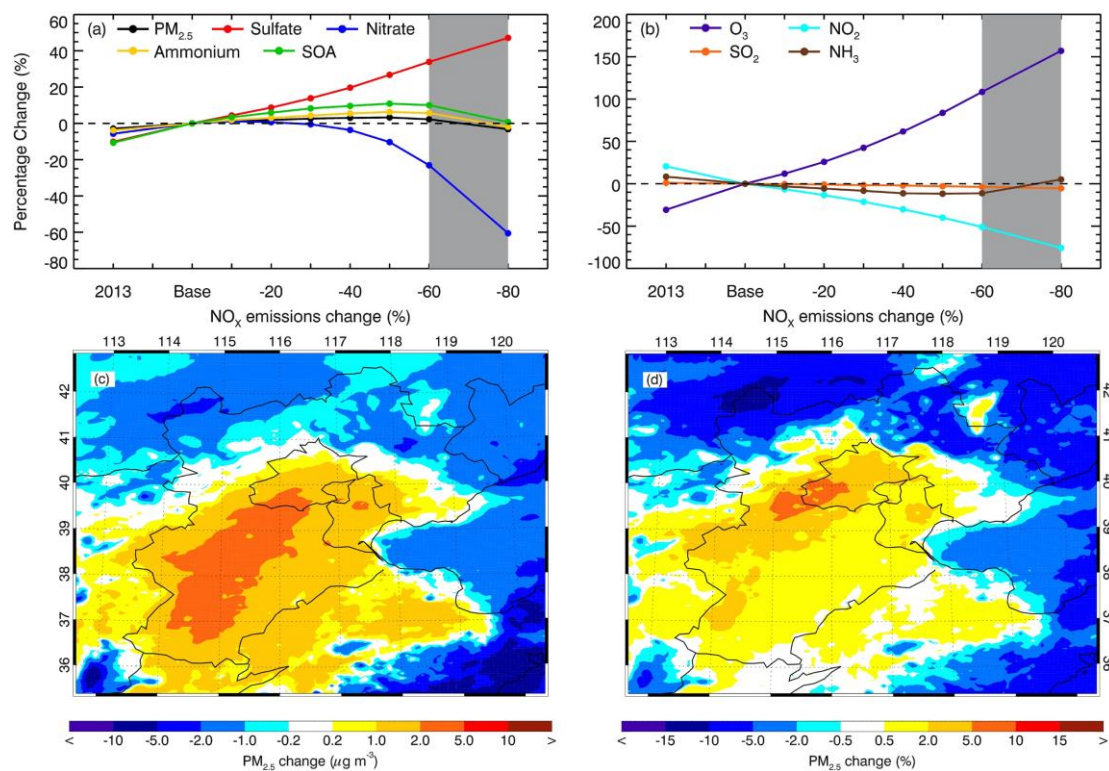
493
494
495
496
497
498
499

Figure 1. Variations of the filter measured average (a) mass concentrations of the PM_{2.5} constituents and (b) their contributions to the PM_{2.5} mass at an urban site in Beijing from 2013 to 2018 during wintertime PM pollution days with PM_{2.5} concentrations exceeding 75 $\mu\text{g m}^{-3}$.



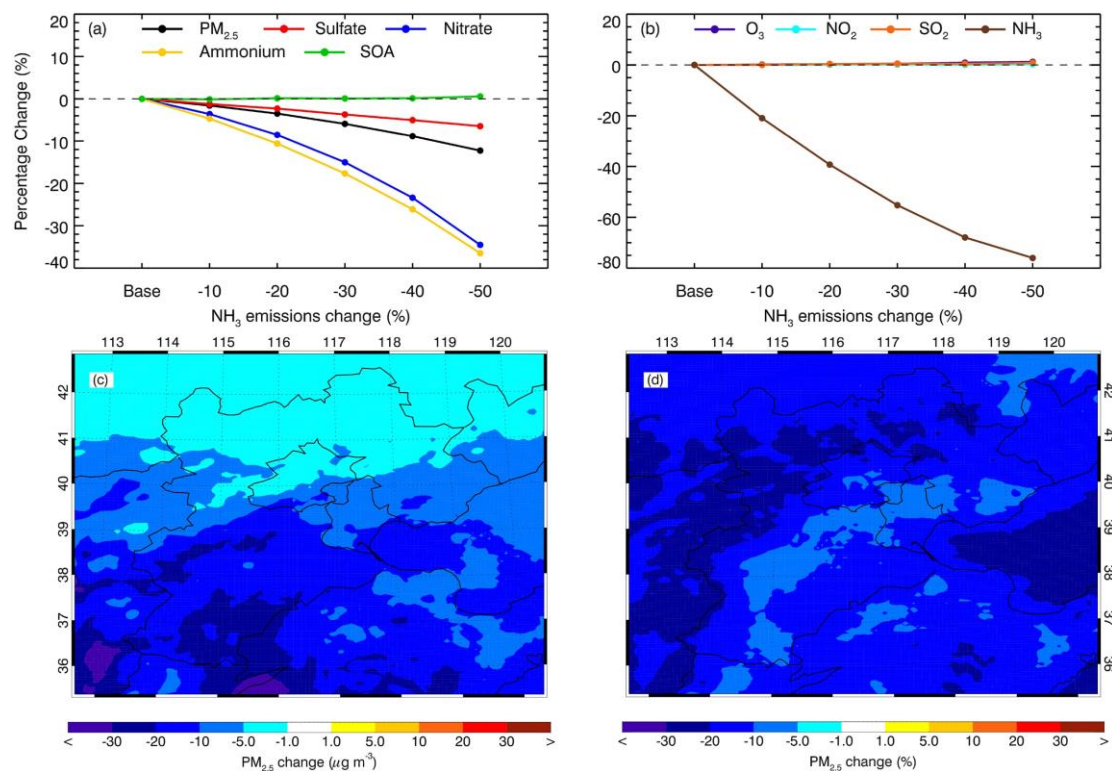
500
501
502
503
504
505

Figure 2. Variations of the filter measured wintertime sulfate, nitrate, and ammonium concentrations from 2014 to 2018 when the PM_{2.5} level exceeds 75 µg m⁻³ in (a) Tianjin, (b) Tangshan, (c) Baoding and (d) Shijiazhuang in the BTH.



506
507
508
509
510
511
512
513
514

Figure 3. Variations of average concentrations of PM_{2.5} and secondary aerosols (a) as well as the gas pollutants (b) in the BTH during the episode with the NO_x emissions changes, and mass (c) and percentage (d) distributions of the PM_{2.5} variation during the simulation period when the NO_x emissions are reduced by 50%. The shading area in (a) and (b) shows the scenario of the NO_x emission reduction during the lockdown period due to the COVID-19 outbreak.



515
516
517
518
519
520
521
522

Figure 4. Variations of average concentrations of PM_{2.5} and secondary aerosols (a) as well as the gas pollutants (b) in the BTH during the episode when the NH₃ emissions are reduced from 10% to 50%, respectively, and mass (c) and percentage (d) distributions of PM_{2.5} reductions when the NH₃ emissions are reduced by 50%.